Finite Element Method Solutions for Semi-linear Elliptic PDEs with critical Sobolev Exponents on Non-spherical 3D Domains

AR HUMPHRIES, Centre for Mathematical Analysis and its Applications, School of Mathematical Sciences, University of Sussex, Brighton, BN1 9QH, UK.

CJ BUDD, School of Mathematics, University of Bath, Claverton Down, Bath BA2 7AY, UK.

AJ WATHEN, Oxford University Computing Laboratory, Numerical Analysis Group, 11 Keble Road, Oxford OX1 3QD, UK.

Presented at Equadiff 95,
Lisbon, Portugal,
24th–29th July 1995.

Abstract. We compute general (non-radial) positive solutions of the semi-linear elliptic PDE $\Delta u + \lambda u + u^5 = 0$, in 3 space dimensions (where the nonlinearity is critical) using the Finite Element Method. We have overcome two fundamental difficulties in this approach. Firstly the convergence of the numerical solutions is very slow (on regular grids) and it is necessary to work with very fine meshes ($\approx 10^6$ nodes). A full Newton iteration is then infeasible, and we have succesfully implemented an approximate Newton method which does not require storage of the full Jacobian, but nevertheless still gives very fast convergence, even when the solution is developing a 'spike.' Secondly, although there is a critical value λ_0 such that there is no positive solution of the PDE for $\lambda < \lambda_0$, the FEM discretization is finite dimensional and variational theory then shows that there exists a numerical solution for *all* $\lambda < \lambda_1$. However using formal asymptotics we can recover information about the solution of the PDE from the numerics and use this to approximate λ_0, in particular obtaining numerical evidence that corroborates McLeod's conjecture, that $\lambda_0 = \lambda_{**}$, in the case Ω is a cube.

1 Introduction

The semi-linear elliptic partial differential equation

$$\left.\begin{array}{ll} \Delta u + \lambda u + u^5 = 0, & \text{on } \Omega \subset \mathbb{R}^3, \\ u > 0 & \text{in } \Omega, \\ u = 0 & \text{on } \partial\Omega. \end{array}\right\} \tag{1}$$

where Ω is a bounded domain in $\mathbb{R}^3$ was first studied by Brezis and Nirenberg [2]. This equation arises out of the Yamabe problem. Its behaviour is delicate because in $\mathbb{R}^3$ the Sobolev embedding $H_0^1(\Omega) \subset L^6(\Omega)$ is not compact. The early work on this problem is reviewed in [1].

Much of the research into this problem has concentrated on the case where Ω is a sphere for then the famous result of Gidas, Ni and Nirenberg [8] implies that the solution is radially symmetric and the problem reduces to an ODE in 1-dimension which is somewhat easier to study than the original problem.

We will study the behaviour on more general domains by computing numerical solutions using the finite element method (FEM). In this paper we will restrict attention to the cube, and give a brief summary of our methods and results. Further details can be found in [6]. More general domains are also considered in [6, 7].

For the case where Ω is a sphere a positive solution bifurcates from the trivial solution at the principal eigenvalue λ_1 of the Laplacian. The bifurcation is to the left, and the solution only exists for $\lambda \in (\lambda_1/4, \lambda_1)$. As $\lambda \to \lambda_1/4$ the solution develops a point singularity at the centre of the sphere and tends pointwise to zero in the rest of the domain. Thus $\|u\|_\infty \to \infty$ as $\lambda \to \lambda_1$, although $\|u\|_{H_0^1}$ remains bounded and $\|u\|_2 \to 0$.

For general star-shaped domains it is shown in [2] that there exists a solution if and only if $\lambda \in (\lambda_0, \lambda_1)$. Here $\lambda_0 > 0$ is unknown for general domains, as is the behaviour of the solution in the limit as $\lambda \to \lambda_0$. For Ω a cube we will compute λ_0 numerically, and the study the behaviour of the solution as $\lambda \to \lambda_0$. We also compute the upper bound λ_{**} for λ_0 which was derived from the Green's function of the linear problem by McLeod [9], and for Ω a cube numerically verify McLeod's conjecture that $\lambda_{**} = \lambda_0$.

In Section 2 we give details of the Finite Element Method used to produce the numerical solutions. In Section 3 we give details of McLeod's conjecture and the computation of λ_{**}. In Section 4 we present numerical results for the full nonlinear problem. The nature of this problem makes the computation of accurate numerical results very difficult, and in Section 5 we use formal asymptotics to improve the numerical solution and verify McLeod's conjecture for the cube.

2 Finite Element Method

We divide the cube (of side 1) Ω into a regular grid of cubic elements of side h. We then let $S_h \subset H_0^1(\Omega)$ be the space of functions which are trilinear on each element, continuous on Ω and vanish on the boundary of Ω. The FEM solution U_h is then defined via the weak formulation of (1):

$$-\langle \nabla U_h, \nabla w \rangle + \langle \lambda U_h + U_h^5, w \rangle = 0 \quad \forall w \in S_h. \tag{2}$$

Let $\{\varphi_i\}_{i=1}^N$ be a basis for S_h composed of functions which take the value 1 at the i^{th} node and 0 at all other nodes (where the nodes are the corners of the elements). Then we may write

$$U_h(x) = \sum_{i=1}^{N} u_i \varphi_i(x) \tag{3}$$

and

$$-\sum_{i=1}^{n} u_i \langle \nabla\varphi_i, \nabla\varphi_j \rangle + \langle \lambda U_h + U_h^5, \varphi_j \rangle = 0 \quad \forall j = 1, \ldots, N. \tag{4}$$

Equivalently

$$KU = G(U, \lambda), \tag{5}$$

where $U = [u_1, \ldots, u_N]^T$ is the vector of unknowns which define the solution (3) and

$$K_{ij} = \langle \nabla\varphi_i, \nabla\varphi_j \rangle, \qquad G(U, \lambda)_i = \langle \lambda U_h + U_h^5, \varphi_i \rangle. \tag{6}$$

We compute the numerical solution by path following in λ, solving (5) at each step. The path following is begun at the bifurcation from the trivial solution using a Lyapunov-Schmidt reduction.

The nonlinearity enters the numerical approximation via the terms $G(U, \lambda)_i$. To compute these terms requires an integration to be performed over Ω. In the FEM product approximation and mass lumping are often used to approximate this term and avoid the need for numerical quadrature. However since the behaviour of (1) depends crucially on the nonlinearity we use 4 point 3D tensor product Gaussian quadrature over each element (ie 64 quadrature points per element) to evaluate this integral *exactly*. An efficient elementation of this procedure is described in [5].

To solve (5) at each step we use an approximate Newton iteration

$$U^{n+1} = U^n - \widetilde{J}^{-1}[KU^n - G(U^n, \lambda)] \tag{7}$$

where $\widetilde{J}$ is an approximation to the Jacobian

$$J = K - G_u(U^n, \lambda). \tag{8}$$

We use fine meshes with up to $N = 10^6$ nodes so that the matrices J and K contain up to 10^{12} entries. However due to the choice of basis for S_h these matrices are sparse. We can obtain all the information needed to construct K by computing the 8×8 matrices $\langle \nabla\varphi_i, \nabla\varphi_j \rangle_e$ over each element e where the $\{\varphi\}_{i=1}^8$ are the 8 basis functions centred at the corners of e, which are not identically zero on that element. Indeed since we use a regular mesh and our basis functions are translations of one another these 8×8 matrices are all identical and so we only need to store one 8×8 matrix to construct K.

The matrix J shares the same sparsity structure as K and the same element matrix approach can be applied. However since J depends on U^n the 8×8 matrices thus defined will all be different, and must all be stored in order to construct J. Although this reduces the storage requirement for J from N^2 to $64N$ entries with $N = 10^6$ this would still require 500MB of memory to store on a computer; which is infeasible on a modern work station. To solve this problem we first approximate J by diagonalizing the nonlinear term $G_u(U^n, \lambda)$ via

$$[LG_u(U^n, \lambda)]_{ii} = \sum_{j=1}^{N} [G_u(U^n, \lambda)]_{ij} \tag{9}$$

and letting

$$\widetilde{J} = K - LG_u(U^n, \lambda). \tag{10}$$

Since $LG_u(U^n, \lambda)$ is diagonal to compute $\widetilde{J}$ from K via (10) requires just N entries of storage.

If U_h is smooth and $\|U_h\|_\infty$ is small the action of $\widetilde{J}$ is a good approximation to the action of J and the approximate Newton iteration typically converges in one iteration. (Note that because we are path following we are able to always start the Newton iteration from a good initial guess.)

Unfortunately we will see later that although U_h is smooth and tending to 0 away from the centre of the cube as λ decreases, at the centre of the cube the numerical solution develops a spike, and the approximate Newton iteration described above fails. However the spike is a local feature and we recover a convergent approximate Newton iteration by modifying the above procedure slightly so that the diagonalization described in (9) is only done for entries corresponding to elements away from the location of the spike, and saving the full 8×8 matrices for elements near the spike. This procedure requires minimal storage and results in an approximate Newton iteration which converges in 1 or 2 iterations. For further details see [5].

3 Green's Function Approach

Let $G_\lambda(x, y)$ be the Green's function for the linearized problem $\Delta u + \lambda u = 0$. Then we may write

$$G_\lambda(x, y) = \frac{1}{4\pi|x-y|} + g_\lambda(x, y) \tag{11}$$

where $g_\lambda(x, y)$ is called the *regular part* of the Green's function. McLeod [9] and Schoen [10] showed independently that if there is a point $x \in \Omega$ such that $g_\lambda(x, x) > 0$ then there exists a solution of (1). Moreover it follows from the Maximum Principle and symmetry arguments that g_λ increases with λ and that for Ω a cube, $g_\lambda(x, x)$ achieves its maximum at the centre of the cube. Thus there exists λ_{**} such that $g_\lambda(0, 0) > 0$ if and only if $\lambda > \lambda_{**}$, and hence that there exists a solution to (1) for $\lambda \in (\lambda_{**}, \lambda_1)$. It follows immediately that $\lambda_{**} \geq \lambda_0$. For Ω a sphere Mcleod showed further that $\lambda_{**} = \lambda_0$, and conjectured that this result would also hold for general star-shaped domains. In Section 5 we present numerical evidence which shows that $\lambda_{**} \approx \lambda_0$ for Ω a cube.

To compute λ_{**} we use the fact (see [6]) that $g_\lambda(x, x) = h_\lambda(x, x)$ where

$$\left.\begin{array}{rll} \Delta h_\lambda(x, y) + \lambda h_\lambda(x, y) = 0, & & x \in \Omega, \\ h_\lambda(x, y) = -\frac{\cos(\lambda^{1/2}|x-y|)}{4\pi|x-y|} & & x \in \partial\Omega. \end{array}\right\} \tag{12}$$

Using (12) and the FEM we can easily compute $g_\lambda(0, 0)$ for any value of λ. Note that since (12) is linear the complications described in Section 2 do not arise here for the FEM. In particular we do not need to perform a Newton iteration; a simple conjugate gradient iteration will solve the linear finite element equations, and also since the right-hand side of (12) vanishes do not need to perform any numerical quadrature. Finally we solve $g_\lambda(0, 0) = 0$ for λ using interval bisection. This reveals very cheaply and quickly that

$$\lambda_{**} \approx 7.5045 \tag{13}$$

for a cube of side 1.

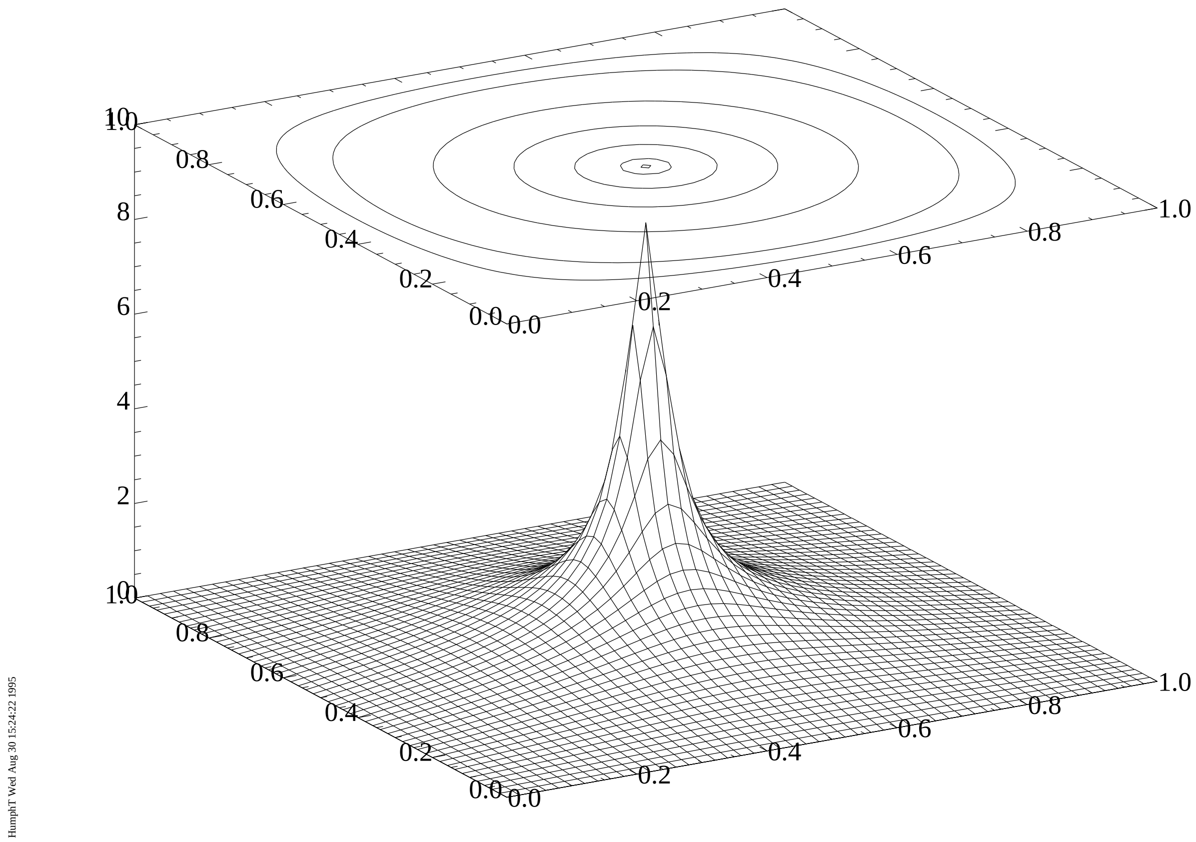

Figure 1: Cross section of numerical solution U_h through centre of cube with $h = 1/100$ and $\lambda = \lambda_{**} = 7.5045$, with contour plot which shows the radial symmetry of the solution in the centre of the domain.

4 Numerical Computations

We present numerical solutions in Figures 1 and 2. The numerical solutions to (2) which we compute are observed to be positive and cubically symmetric on Ω; neither of conditions was imposed apriori on the numerics. Figure 1 clearly shows that the numerical solution develops a spike at the centre of the cube. Moreover this spike appears to be roughly spherically symmetric. Away from the spike, $U_h \sim 0$.

Figure 2 shows how $\|U_h\|_\infty$ varies as the mesh is refined. For $\lambda > 13$ all the plots agree, indicating that the numerics have converged and are giving a good approximation to the solution u to the underlying problem (1). However for $\lambda < 10$ the plots all disagree indicating that even on our finest mesh of $h = 1/100$, or $N = 10^6$ nodes, the numerical solution U_h of (2) has not converged to the solution of (1). Moreover, we can compute solutions of (2) all the way back to $\lambda = 0$, whereas we know from [2] that there exists a $\lambda_0 > 0$ such that (1) has no solution for $\lambda < \lambda_0$. Thus for λ sufficiently small ($\lambda < \lambda_0$) the numerical solutions are spurious; they do not correspond to any solution of the underlying equation (1).

The problem with the numerics is of coarse that the interesting behaviour for (1) results from the criticality of the Sobolev embedding; whilst the numerical solution is computed in a

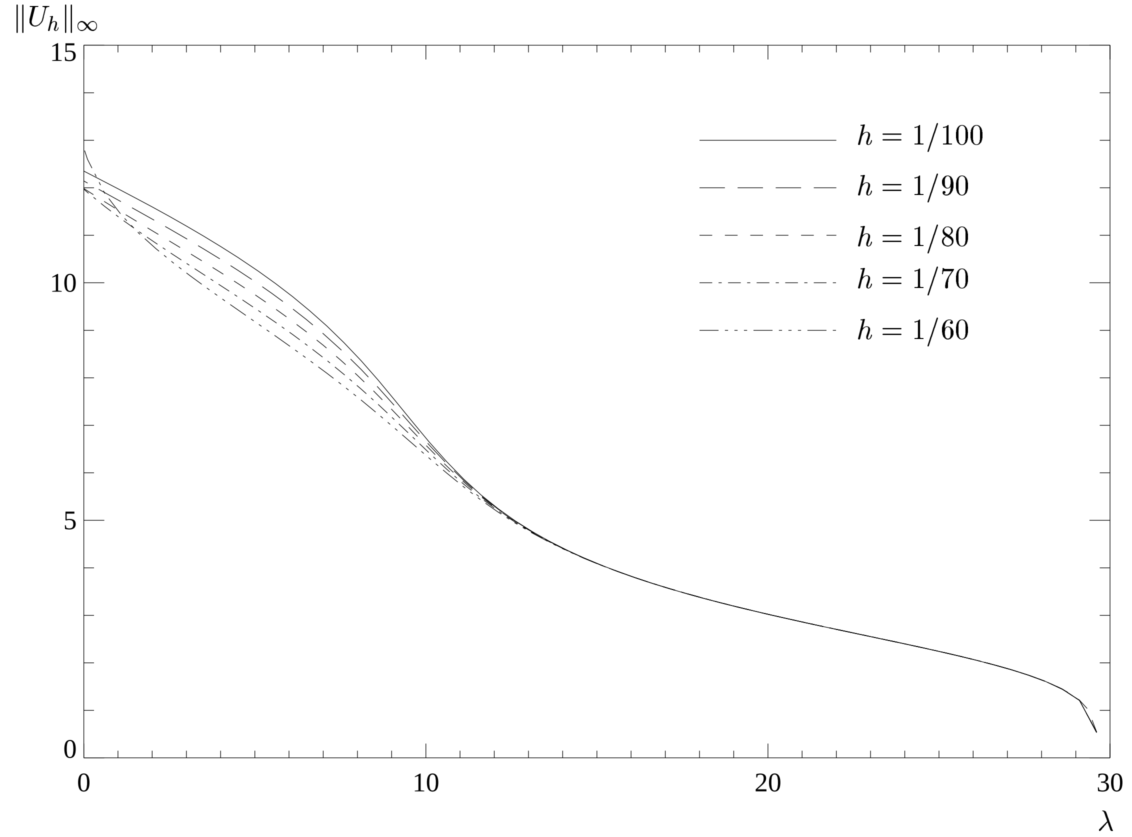

Figure 2: Graph of $\|U_h\|_\infty$ against λ, for grids varying between $h = 1/60$ and $h = 1/100$.

finite dimensional subspace where all norms are equivalent. It might seem at this point that our approach of tackling (1) numerically has failed, however we will show in the final section how to use our numerics to estimate $\|u\|_\infty$ and λ_0.

5 Asymptotic Theory and Results

In [4] a formal asymptotic theory is developed for finite element approximations to (1) on the sphere. This theory is extended to cuboid domains in [6]. There is insufficient space to reproduce the theory here but the basis is as follows. For sufficiently fine meshes and smallish values of λ we find that within the spike $u^5 \gg \lambda u$ whilst away from the spike $\lambda u \gg u^5$. Thus within the spike we would expect the solution to resemble that of $\Delta u + u^5 = 0$. This equation has well known ground states solutions on $\mathbb{R}^3$: for any $\gamma > 0$, $u = w_\gamma$ is a solution where

$$w_\gamma(x) = \frac{\gamma}{\sqrt{1 + \frac{\gamma^4 \|x\|^2}{3}}}, \tag{14}$$

with $\|w_\gamma\|_\infty = \gamma$. Away from the spike we would expect the solution to resemble that of $\Delta u + \lambda u = 0$; ie. to be some multiple of the Green's function.

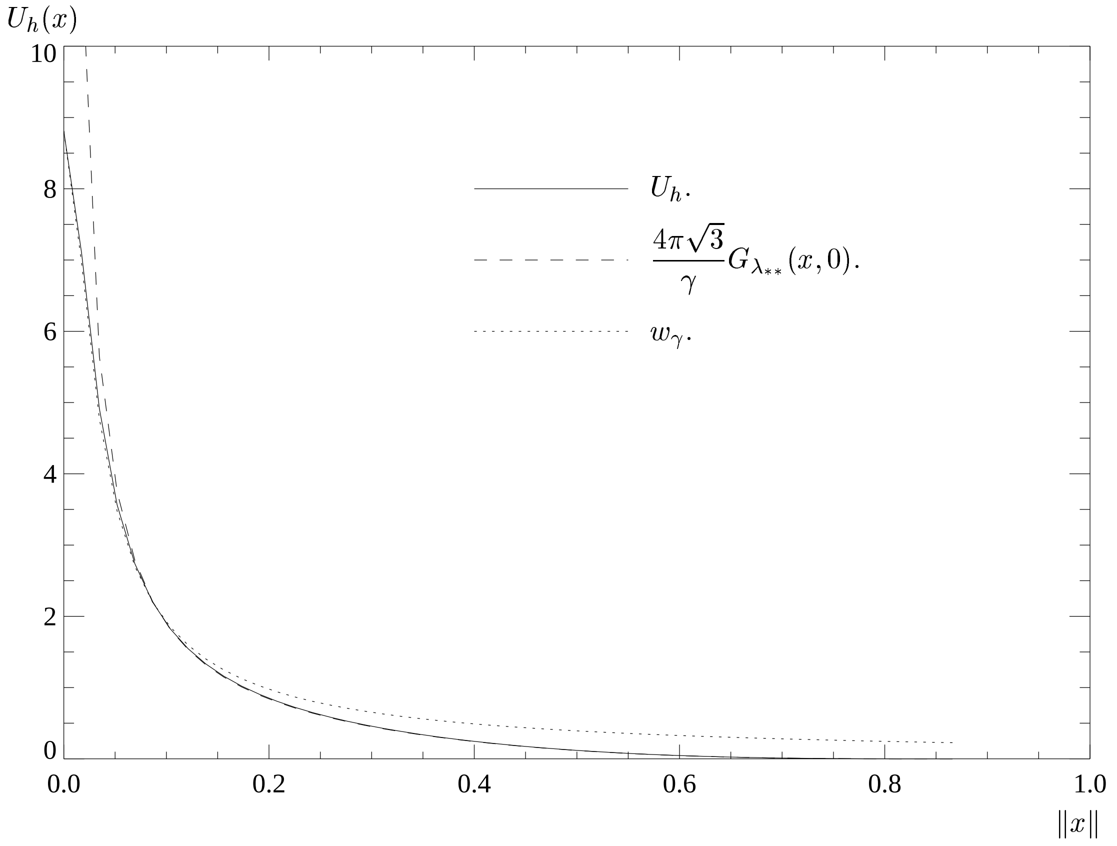

Figure 3: Graph of $U_h(x)$ against $\|x\|$ along the long diagonal $x = y = z$ of the cube, with $h = 1/100$ and $\lambda = \lambda_{**} = 7.5045$. Also plotted are the ground state solution $w_\gamma(x)$ (14) with $\gamma = \|U_h\|_\infty$, and a scaling of the Green's function (11) of the linearized problem.

As we see in Figure 3 there is a region near to the spike where both approximations are good, and a matching argument then reveals that away from the spike

$$u(x) \approx \frac{4\pi\sqrt{3}}{\|u\|_\infty} G_\lambda(x,0). \tag{15}$$

Formal analysis based around these ideas yields a number of useful formulae. For $\lambda > \lambda_0$ we find that asymptotically as $h \to 0$

$$\|u\|_\infty \sim \frac{\|U_h\|_\infty}{(1 - Ch^2\|U_h\|^8)^{\frac{1}{2}}}, \tag{16}$$

where C is a constant of order 10^{-4}. Whilst for $\lambda = \lambda_0$

$$\|U_h\|_\infty \sim Kh^{-1/4}. \tag{17}$$

This second formula reveals why $\|U_h\|_\infty$ is increasing so slowly in Figure 2 as h is refined. Note that since the $N = 1/h^3$, equation (17) states that $\|U_h\|_\infty \sim KN^{1/12}$; so increasing the number of nodes N has little effect on the numerics.

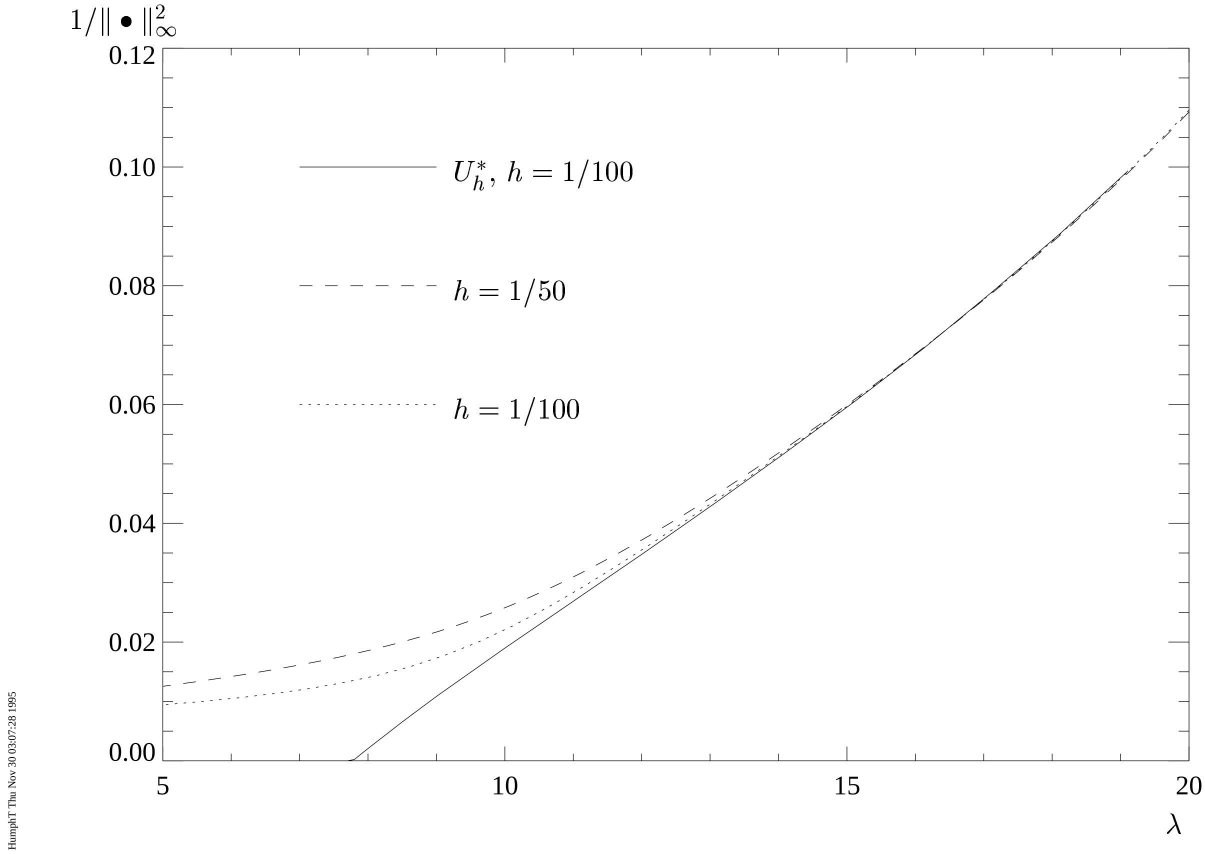

Figure 4: Graphs of $1/\|U_h\|_\infty^2$ for $h = 1/50$, $1/100$ together with the extrapolated value $1/\|U_h^*\|_\infty^2$ for $h = /100$ plotted against λ.

Using our numerical results from our finest meshes ($h = 1/90$, $1/100$) we can eliminate $\|u\|_\infty$ from (16) and estimate

$$C = 3.3 \times 10^{-4}.$$

Now using this value of C in (16) from $\|U_h\|_\infty$ we can compute a better approximation $\|U_h^*\|_\infty$ to $\|u\|_\infty$. This is illustrated in Figure 4. Note that $\|U_h^*\|_\infty^{-2}$ is roughly a straight line, which is consistent with the result of [3] that for Ω a sphere, $\|u\|_\infty^{-2} \sim m(\lambda - \lambda_0)$ and lends further confidence to our results.

From the intersection with the x-axis we also obtain the immediate estimate that $\lambda_0 \approx 7.8$. However because (16) is an asymptotic formula for small h, and even our finest mesh with $N = 10^6$ has $h = 1/100$ and so is still relatively coarse, and moreover we have also used the numerics to estimate the constant C, we can only say with confidence that $\lambda_0 \in (7, 8)$. This is consistent with $\lambda_0 = \lambda_{**}$ which would confirm McLeod's conjecture for this domain. In [6] we are able to perform a more detailed analysis of the numerics and obtain an estimate for λ_0 which is much closer to λ_{**}.

6 Concluding Remarks

Computing accurate numerical approximations to the solution of (1) is difficult, nevertheless we have shown that some progress can be made using this approach. As mentioned already, a more detailed study of this problem is contained in [6], where general cuboid and in particular long thin domains are also considered. The asymptotic theory was originally derived for the radial case [4]. Further details of the numerics are contained in [5]. The forthcoming paper [7] will consider non-convex and non-starshaped domains where the behaviour of (1) becomes even more interesting.

Acknowledgements

This work was begun when all three authors were at the School of Mathematics, University of Bristol, UK. We are also grateful to the EPSRC for financial support.

References

[1] H. Brezis. Elliptic equations with limiting Sobolev exponents – the impact of topology. *Comm. Pure Appl. Math.*, 39:S17–S39, 1986.

[2] H. Brezis and L. Nirenberg. Positive solutions of nonlinear elliptic equations involving critical Sobolev exponents. *Comm. Pure Appl. Math.*, 36:437–477, 1983.

[3] H. Brezis and L.A. Peletier. Asymptotics for elliptic equations involving critical growth. In *Partial Differential Equations and the Calculus of Variations, Volume I*, pages 149–192. Birkhäuser, 1989.

[4] C.J. Budd and A.R. Humphries. Numerical approximations of radial solutions of semi-linear elliptic PDEs with near critical exponents. Mathematics Research Report no AM-95-07, University of Bristol, 1995.

[5] C.J. Budd, A.R. Humphries, and A.J. Wathen. Finite element solutions for semi-linear elliptic PDEs on large 3D grids, 1995. In preparation.

[6] C.J. Budd, A.R. Humphries, and A.J. Wathen. Numerical approximations of non-radial solutions of semi-linear elliptic PDEs with critical exponents, 1995. In preparation.

[7] C.J. Budd, A.R. Humphries, and A.J. Wathen. Numerical approximations of solutions of semi-linear elliptic PDEs with critical exponents on non-convex and non-starshaped domains, 1995. In preparation.

[8] W-M. Gidas, B. Ni and L. Nirenberg. Symmetry and related properties via the maximum principle. *Comm. Math. Phys.*, 68:209–243, 1979.

[9] B. McLeod. A nonlinear elliptic equation with critical Sobolev exponent, 1984. Unpublished work.

[10] R. Schoen. Conformal deformation of a Riemannian metric to constant scalar curvature. *J. Diff. Geom.*, 20:479–495, 1984.